

DSC STUDIES ON THE KINETICS OF DECOMPOSITION OF MANGANESE DIOXIDE *

CHEN QIYUAN and CHEN XINMIN

Department of Chemistry, Central South University of Technology, Changsha, Hunan (People's Republic of China)

(Received 22 January 1987)

ABSTRACT

The kinetics of the thermal decomposition of manganese dioxide are studied with the DSC method. A non-isothermal reaction model consisting of two stages linked by the basic equation of interface reaction control is derived and the model agrees very well with the course of this decomposition reaction almost over the full range of reaction. Kinetic parameters for this reaction are calculated using this model and the methods of Kissinger, Duswalt and Ozawa.

INTRODUCTION

Various types of thermal analysis have been applied in almost all fields of material research, and non-isothermal calorimetric techniques (DTA and DSC) are rapidly becoming a valuable tool for obtaining kinetic data in a large variety of phase transformations and other processes. Recently the DSC technique has become more important in kinetic research for its quantification of heat effects. However, few of these methods can ideally be applied to reactions which contain more than one stage, such as the decompositions of most metal oxides. The purpose of this paper is to present a non-isothermal model containing more than one stage and to make a DSC study of the kinetics of the decomposition of manganese dioxide using this model.

Previous studies [1–4] on the kinetics of the decomposition of manganese dioxide have been reported, but few of them deal with the reaction mechanism in detail. The aim of the present work is to study the kinetics of the decomposition of manganese dioxide and to determine the detailed mechanism as well as the relevant kinetic parameters.

* Paper presented at the Sino-Japanese Joint Symposium on Calorimetry and Thermal Analysis, Hangzhou, People's Republic of China, 5–7 November 1986.

THEORY AND DERIVATION

It is well known that the decomposition of metal oxides can be divided into three stages [5]. In the first stage (stage I), nuclei form and some of them, with sizes exceeding a certain critical value, can grow and are called growth nuclei. The growth nuclei grow and overlap each other in the second stage (stage II). This process goes on until the reaction accelerates to the maximum rate. Then it reaches the third stage (stage III) and slows down until the end (see Fig. 1). The first stage is too complex for modelling and the data from DSC are not accurate enough since the values are very small. Thus, our modelling considers the second and the third stages.

For the decomposition of metal oxides, the following hypotheses are usually considered to be reasonable:

(1) The solid product of decomposition is not compact and the diffusion resistance of the product layer can be neglected.

(2) The interface reaction is of zero order, i.e.

$$-\frac{dW}{dt} = kA \quad (1)$$

where W is the weight of reactant, t is time, A is the total area of the interface and k is the specific rate which may be expressed as

$$k = Z e^{-E_a/RT}$$

where Z is the frequency factor, E_a is the activation energy, R is the gas constant and T is the absolute temperature.

Once a number of growth nuclei form at the interface, the second stage begins and eqn. (1) will become

$$-\frac{dW}{dt} = ksN_0 \quad (2)$$

where s is the area of the hemispherical surface of each growth nucleus and N_0 is the number of growth nuclei.

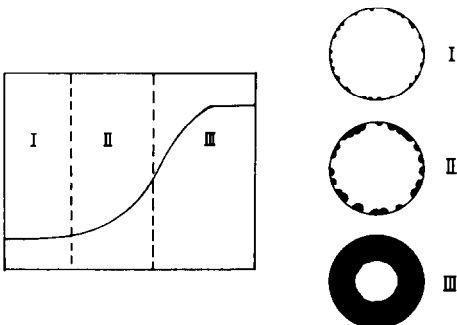


Fig. 1. Scheme of the mechanism of heterogeneous reaction consisting of three stages.

Considering the relationships $s = 2\pi\hat{r}^2$, where \hat{r} is the radius of each growth nucleus; $\alpha = (W_0 - W)/W_0$, where α is the reacted fraction and W_0 is the initial weight of reactant; $W_0 = \frac{4}{3}\pi R_0^3\rho$, where R_0 is the initial radius of the particle and ρ is the density of reactant; and $\beta = dT/dt$, where β is the heating rate, then from eqn. (2) it follows that

$$\frac{d\alpha}{dT} = \frac{3Z}{R_0\rho\beta} \left(\frac{N_0}{2}\right)^{1/3} e^{-E_a/RT} \alpha^{2/3} \quad (3)$$

However, during growth, some overlap between nuclei takes place. Therefore eqn. (3) should be rewritten as

$$\frac{d\alpha}{dT} = \frac{3Z}{R_0\rho\beta} \left(\frac{N_0}{2}\right)^{1/3} e^{-E_a/RT} \alpha^{2/3} \left(1 - \frac{\alpha}{\alpha_t}\right) \quad (4)$$

where α_t is the reacted fraction when the whole surface of a particle has just been covered with product.

Let $K' = \frac{3Z}{R_0\rho} \left(\frac{N_0}{2}\right)^{1/3}$, then eqn. (4) becomes

$$\frac{d\alpha}{dT} = \frac{K'}{\beta} e^{-E_a/RT} \alpha^{2/3} \left(1 - \frac{\alpha}{\alpha_t}\right) \quad (5)$$

Let $l = (\alpha/\alpha_t)^{1/3}$, then on integration of eqn. (5) gives

$$F(l) - F(l_1) = \frac{K'}{\alpha_t^{1/3}\beta} \int_{T_1}^T e^{-E_a/RT} dT \quad (6)$$

This is the kinetic equation of stage II, where l_1 and T_1 are the l function and T respectively at the beginning of stage II, and

$$F(l) = \int \frac{3 dl}{1-l^3} = \ln \frac{\sqrt{1+l+l^2}}{1-l} + \sqrt{3} \arctan \frac{2l+1}{\sqrt{3}}$$

In stage III, considering eqn. (1) and $A = 4\pi r^2$, the rate equation will be

$$\frac{d\alpha}{dT} = \frac{3Z}{R_0\rho\beta} e^{-E_a/RT} (1-\alpha)^{2/3} \quad (7)$$

where r is the radius of the unreacted nucleus of the particle. Let $K = Z/R_0\rho$, then

$$\frac{d\alpha}{dT} = \frac{3K}{\beta} e^{-E_a/RT} (1-\alpha)^{2/3} \quad (8)$$

Integration gives

$$(1-\alpha_2)^{1/3} - (1-\alpha)^{1/3} = \frac{K}{\beta} \int_{T_2}^T e^{-E_a/RT} dT \quad (9)$$

where α_2 and T_2 are the reacted fraction and the absolute temperature respectively at the beginning of stage III.

From the definitions of K' and K , it can be shown that $K'/K = 3(N_0/2)^{1/3}$ and thus, $N_0 = 2(K'/3K)^3$.

EXPERIMENTAL

A SETARAM differential scanning calorimeter (DSC-111) was used for the present kinetic study. The temperature and sensitivity had been carefully calibrated before the experiments. Heating rates were $0.5^{\circ}\text{C min}^{-1}$, $1.3^{\circ}\text{C min}^{-1}$, $2^{\circ}\text{C min}^{-1}$, $3^{\circ}\text{C min}^{-1}$ and $5^{\circ}\text{C min}^{-1}$ respectively. The full scale of the amplifier was 1 mV. In each run, a sample (100 ± 0.5 mg) was placed as a shallow layer in a platinum boat, over which a constant current of pure argon was passed to remove the oxygen given out in the decomposition of the oxide. In order to guarantee the identity of conditions, five runs were carried out at a stretch after prolonged stabilizing.

The test samples were spectroscopically pure manganese dioxide powder, which was affirmed as $\beta\text{-MnO}_2$ by X-ray diffraction and as having the stoichiometric composition by gravimetric analysis. Sieving of the dried powder provided specimens of uniform size (0.0425 ± 0.0025 mm).

An HP personal computer (HP-85A) was used on line to collect and store the experimental data amounting to about 2400–4500 points. Then, the stored data were processed with another personal computer (HP-87XM) using a special program developed by us.

DATA PROCESSING AND RESULTS

The data processing consisted of three steps. First, five $d\alpha/dT-T$ curves were given after base line correction and relevant $\alpha-T$ curves (e.g. Fig. 2) were obtained by integrating the former.

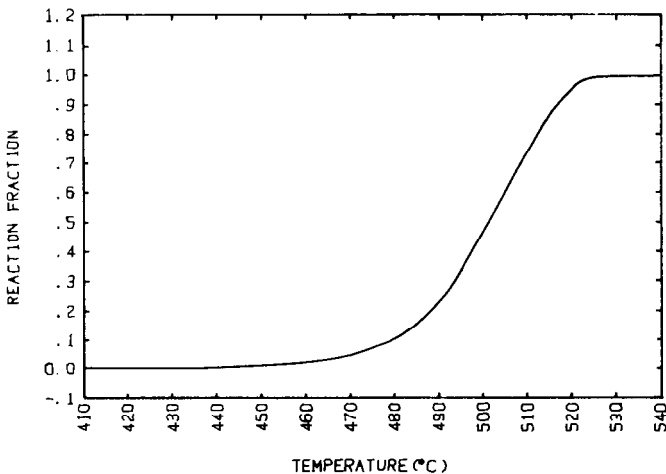


Fig. 2. The $\alpha-T$ curve of the decomposition of MnO_2 .

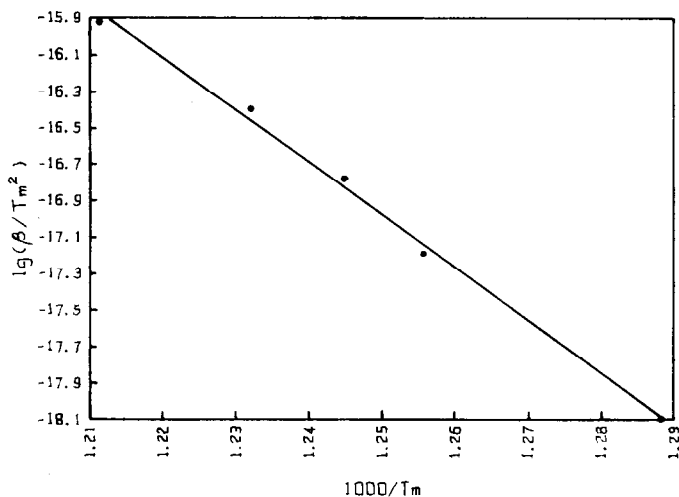


Fig. 3. The $\lg(\beta/T_m^2)-1/T_m$ curve for calculating E_a by Kissinger's method.

Then, the activation energy of the reaction was estimated by the methods of Kissinger [6], Duswalt [7] and Ozawa [8].

According to Kissinger's method [6], the activation energy, $240.4 \text{ kJ mol}^{-1}$, was obtained from the slope of the plot of $\ln(\beta/T_m^2)$ vs. $1/T_m$ (see Fig. 3), where T_m is the peak temperature, the slope is $-E_a/R$ and the linear correlation coefficient is -0.9977 .

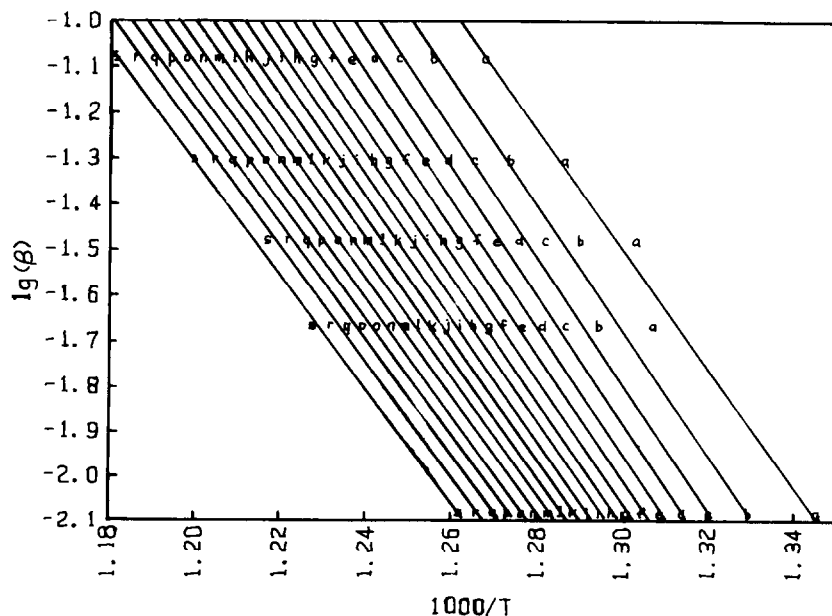


Fig. 4. The $\lg \beta - 1/T$ curves for calculating E_a by Ozawa's method.

TABLE 1

The values of the activation energy of decomposition of MnO_2 (with Ozawa's method)

α	E_a (kJ mol^{-1})	R	α	E_a (kJ mol^{-1})	R
0.05	237.2	-0.9916	0.55	241.5	-0.9969
0.10	248.9	-0.9927	0.60	239.5	-0.9971
0.15	253.3	-0.9937	0.65	237.7	-0.9973
0.20	254.1	-0.9943	0.70	235.8	-0.9974
0.25	253.5	-0.9950	0.75	233.8	-0.9976
0.30	251.9	-0.9953	0.80	232.3	-0.9978
0.35	250.1	-0.9958	0.85	230.6	-0.9978
0.40	248.1	-0.9961	0.90	229.4	-0.9981
0.45	246.0	-0.9963	0.95	227.5	-0.9982
0.50	243.9	-0.9966			

The value of the activation energy from Duswalt's method [7] was $240.3 \text{ kJ mol}^{-1}$, which was obtained by iteration. The initial value of the activation energy was obtained from the formula

$$E_i = -2.19R \left[\frac{d \log \beta}{d(1/T_m)} \right]$$

and the iterated values were obtained using

$$X_i = \frac{E_i}{RT_m} \quad D_i = \frac{2}{x_i} + 1 \quad E_{i+1} = \frac{2.303R}{D_i} \left[\frac{d \log \beta}{d(1/T_m)} \right]$$

The values of the activation energy at various values of α were obtained

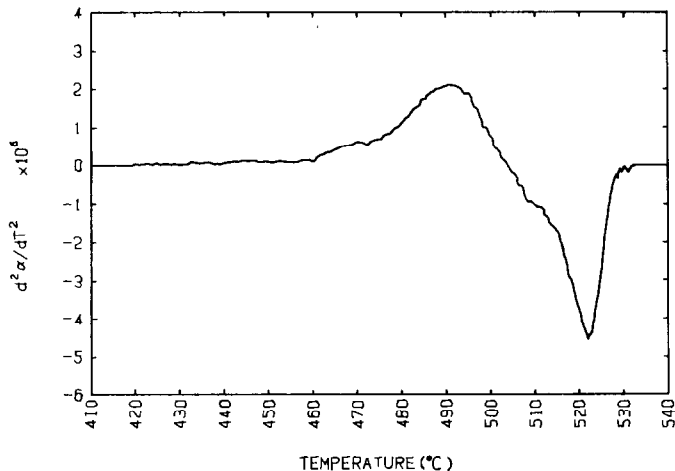


Fig. 5. The $d^2\alpha/dT^2 - T$ curve for the decomposition of MnO_2 .

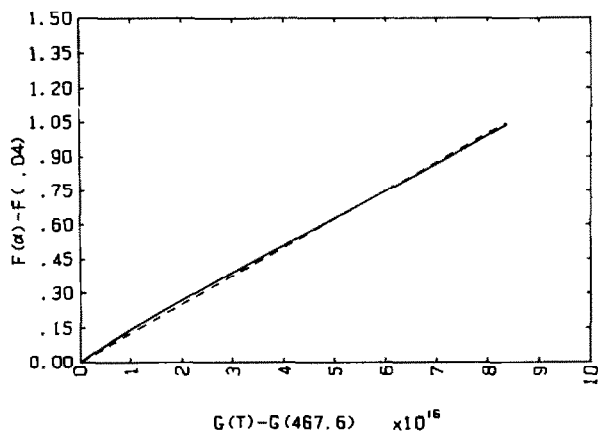


Fig. 6. The linear relationship in stage II of the decomposition of MnO_2 .

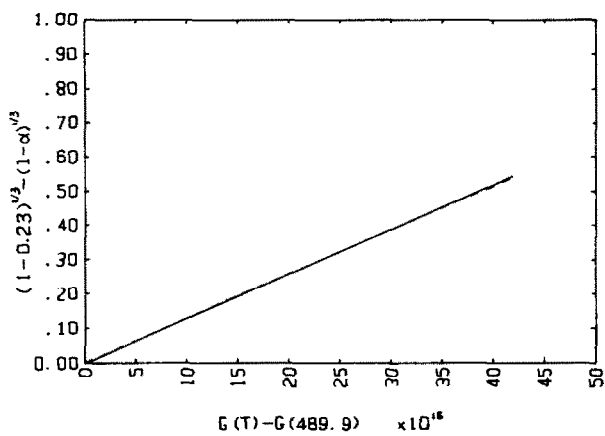


Fig. 7. The linear relationship in stage III of the decomposition of MnO_2 .

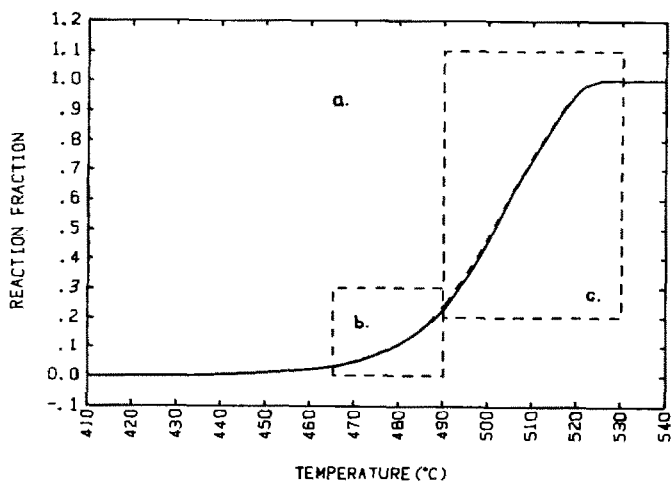


Fig. 8. The decomposition curve of MnO_2 .

TABLE 2
The kinetic analysis results of the decomposition of manganese dioxide

$\beta(^{\circ}\text{C min}^{-1})$	α_t	Range of α	$K' \times 10^{-5}$	R	Range of α	$K \times 10^{-4}$	R	K'/K	N_0
0.5	0.550	0.04-0.231	1.254	0.99977	0.231-0.951	1.290	0.99997	9.719	68
1.3	0.542	0.04-0.189	1.351	0.99985	0.189-0.949	1.155	0.99989	11.697	119
2.0	0.583	0.04-0.180	1.746	0.99908	0.180-0.951	1.279	0.99978	13.649	188
3.0	0.528	0.04-0.176	1.622	0.99918	0.176-0.950	1.128	0.99959	14.385	220
5.0	0.564	0.04-0.168	1.623	0.99911	0.168-0.951	1.069	0.99962	15.182	259
Average:	0.553	0.04-0.189	1.519	0.99940	0.189-0.950	1.184	0.99977	12.828	156
	± 0.021	± 0.025	± 0.207			± 0.097			

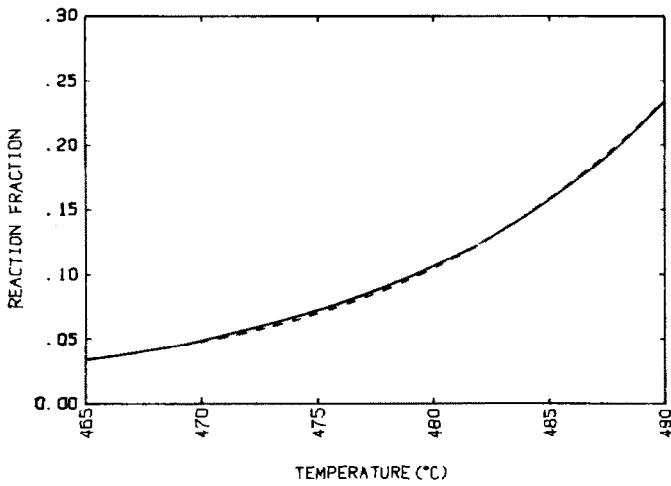


Fig. 9. The decomposition curve of MnO_2 (stage II).

with Ozawa's method [8] using the basic equation

$$\ln \beta = \left[\log \frac{AE_a}{R} - \log g(\alpha) - 2.315 \right] - 0.4567 \frac{E_a}{RT} \quad (10)$$

The results from the slopes of the plots of $\log \beta$ vs. $1/T$ at various values of α (see Fig. 4) are shown in Table 1.

The weighted average of the above three results is 241 kJ mol^{-1} .

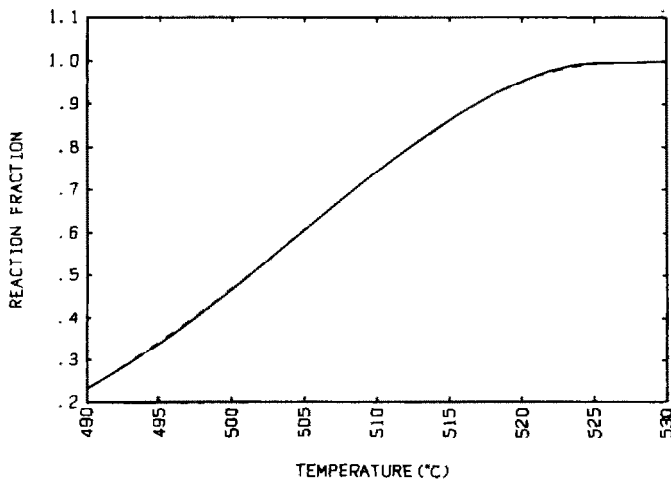


Fig. 10. The decomposition curve of MnO_2 (stage III): - - - - -, calculated results; ———, experimental results.

Before substituting the value of the activation energy in eqns. (6) and (9) to calculate the values of K' and K , the ranges suitable for each equation have to be determined. Calculating the derivatives of $d\alpha/dT$ with respect to T gave $d^2\alpha/dT^2-T$ curves (e.g. Fig. 5). It was shown by calculation that each $F(1-F(l_1))$ was directly proportional to $1/(\alpha_1^{1/3}\beta) \int_{T_1}^T e^{-E_a/RT} dT$ in the range of α between 0.04 and the value corresponding to the maximum of $d^2\alpha/dT^2$ i.e. 0.168–0.231, and each $(1-\alpha_2)^{1/3} - (1-\alpha)^{1/3}$ was directly proportional to $1/\beta \int_{T_2}^T e^{-E_a/RT} dT$ in the range of α between the values corresponding to the maximum and minimum of $d^2\alpha/dT^2$. The values of K' are the slopes of the former, and the linear correlation coefficients (R) are better than 0.999 (e.g. Fig. 6). The values of K are the slopes of the latter, and the linear correlation coefficients are better than 0.9995 (e.g. Fig. 7). The results are shown in Table 2.

Finally, substituting the values of K' and K in eqns. (6) and (9) in the corresponding stages gave five $\alpha-T$ curves which agreed very well with the experimental curves (e.g. Figs. 8–10).

CONCLUSIONS

(1) The values of the activation energy found using the different methods are very close. Thus, the result from these values should be reliable.

(2) Instead of using the usual processing methods, we processed the reaction as stages which were different but related to each other through eqn. (1). Then some interesting conclusions could be drawn from Table 2. Firstly, the reaction mechanism is independent of the heating rate and the present processing method is reliable, since the values for K' and K from runs with different heating rates are very close. Secondly, it is reasonable that the value of N_0 , which can be considered as the number of the growth nuclei at the beginning of stage II, increases with heating rate because of the higher temperature.

(3) Data based on the present non-isothermal reaction model of two stages linked by the basic equation of interface reaction control agreed very well with the experimental results of the decomposition of manganese dioxide in the reaction fraction range of 0.04–1.00. In principle, this model is also usable for other thermal decompositions of a porous solid product.

ACKNOWLEDGEMENT

This work is part of a project supplied by the Science Fund of the Chinese Academy of Sciences.

REFERENCES

- 1 V.G. Vlasov and V.A. Kozlov, *Zh. Fiz. Khim.*, 32 (1958) 2608.
- 2 H.G. Wiedemann and R. Giovanoli, *Calorim. Anal. Therm.*, 13 (1982) I.11.71; *Chem. Abst.*, 97 (1982) 79772.
- 3 K. Terayama and M. Ikeda, *Trans. Jpn. Inst. Met.*, 24 (1983) 754.
- 4 H. Koga, *Nippon Kagaku Kaishi*, 12 (1981) 1939.
- 5 Q. Han, *Kinetics of Metallurgical Process*, Metallurgical Industry Press, Beijing, 1983, p. 52.
- 6 H.E. Kissinger, *J. Res. Nat. Bur. Stand.*, 57 (1956) 217.
- 7 A.A. Duswalt, *Thermochim. Acta*, 8 (1974) 57.
- 8 T. Ozawa, *Bull. Chem. Soc. Jpn.*, 38 (1965) 1881.